

# 000 VRPRM: PROCESS REWARD MODELING VIA VISUAL 001 REASONING 002

003 **Anonymous authors**

004 Paper under double-blind review

## 005 ABSTRACT

006  
007  
008  
009  
010  
011 Process Reward Model (PRM) is widely used in the post-training of Large Lan-  
012 guage Model (LLM) because it can perform fine-grained evaluation of the reason-  
013 ing steps of generated content. However, most PRMs lack long-term reasoning  
014 and deep thinking capabilities. On the other hand, although a few works have  
015 tried to introduce Chain-of-Thought (CoT) capability into PRMs, the annotation  
016 cost of CoT-PRM data is too expensive to play a stable role in various tasks. To  
017 address the above challenges, we propose VRPRM, a process reward model via  
018 visual reasoning, and design an efficient two-stage training strategy. Experimental  
019 results show that using only 3.6K CoT-PRM Supervised Fine-Tuning(SFT) data  
020 and 50K non-CoT PRM Reinforcement Learning (RL) training data, VRPRM can  
021 surpass the non-thinking PRM with a total data volume of 400K and achieved a  
022 relative performance improvement of up to 118% over the base model in the BoN  
023 experiment. This result confirms that the proposed combined training strategy can  
024 achieve higher quality reasoning capabilities at a lower data annotation cost, thus  
025 providing a new paradigm for PRM training with more efficient data utilization.

## 026 1 INTRODUCTION

027 Reward Models (RMs) are a core component in the post-training process of Large Language Models  
028 (LLMs) through Reinforcement Learning with Human Feedback (RLHF). However, most current  
029 reward models are Outcome Reward Models (ORMs) that are oriented towards evaluating the final  
030 result. They can only provide a holistic score for the entire generated content, making it difficult  
031 to supervise the critical reasoning steps and internal logical structure of the generation process. As  
032 a result, they fail to provide stable reward signals about the quality of the reasoning chain during  
033 reinforcement learning.

034 Therefore, an increasing number of Process Reward Models (PRMs) have been proposed to directly  
035 score each step of the generated content. Yet, they face a critical problem: how can a reward model  
036 that lacks reasoning ability itself be used to guide a thinking policy model?

037 To address the poor capability and generalization of reward models, many works on Chain-of-  
038 Thought Reward Models (CoT-RMs) have been proposed. As shown in Fig 1, the vast majority  
039 of these are CoT-ORM models, with only a few study Zhao et al. (2025) training a PRM by syn-  
040 thetizing CoT-PRM supervised fine-tune (SFT) data, which rely on manual annotation or costly  
041 distillation methods. This data bottleneck has become a key obstacle hindering the improvement of  
042 PRM performance and generalization across multiple tasks and scenarios.

043 RL presents a promising approach to not only address the data cost problem but also enhance gener-  
044 alization capabilities beyond what supervised fine-tuning can achieve Chen et al. (2025a); Chu et al.  
045 (2025). As shown in the Fig 2, previous studies typically used outcome-level data for reinforcement  
046 learning, where result-based rewards encourage the model to guess the correct answer, enabling easy  
047 reward through guessing. In contrast, training with process-level data requires evaluating the entire  
048 process, with higher scores awarded only for correctly predicting all steps. This reduces the reliance  
049 on random guesses, promoting more accurate and structured process evaluation.

050 In this paper, we propose Visual Reasoning PRM (VRPRM), a first visual PRM with CoT capability,  
051 and we design an efficient two-stage training data leveraging strategy. First, supervised fine-tuning  
052 (SFT) is performed using a small amount of high-quality CoT-PRM data to activate the model's

	Reward Model	PRM	MM	CoT	RL
054	RRM Guo et al. (2025)			✓	
055	RM-R1 Chen et al. (2025a)			✓	✓
056	Think-RM Hong et al. (2025)			✓	
057	R1-Reward Zhang et al. (2025a)	✓		✓	
058	UnifiedReward Wang et al. (2025c)			✓	
059	Qwen-Math-PRM Zhang et al. (2025b)	✓			
060	GenPRM Zhao et al. (2025)	✓		✓	
061	VisualPRM Wang et al. (2025b)	✓	✓		
062	<b>VRPRM (ours)</b>	✓	✓	✓	✓

Figure 1: The comparison of different RMs. Our VRPRM is the first multi-modal PRM with advanced reasoning capabilities enhanced through RL scaling. **MM** represents whether the RM is multi-modal. **CoT** represents whether the RM has thinking capability. **RL** represents whether reinforcement learning is used when training the model.

initial long-term reasoning and process evaluation capabilities; then, non-CoT PRM data is used to perform reward verification in reinforcement learning, reducing the demand for CoT-PRM data and further enhancing the model’s deep thinking ability. Experimental results show that using only 3.6K CoT-PRM SFT data and 50K non-CoT PRM RL training data, VRPRM can surpass the non-thinking PRM with a total data volume of 400K. This result confirms that the proposed combined training strategy can achieve higher quality reasoning capabilities at a lower data annotation cost, thus providing a new paradigm for PRM training with more efficient data utilization.

Our contributions can be summarized as follows:

- **Pioneering the Integration of CoT RL in Visual PRMs.** We are among the first to systematically address the need for deep thinking in PRMs. We introduce VRPRM, the first-ever multimodal CoT-PRM trained by RL, explicitly designed to enhance the fine-grained reasoning and evaluation capabilities of reward models.
- **A Data-Efficient Two-Stage Training Strategy.** This method demonstrates remarkable data efficiency, enabling our model to surpass a traditional PRM trained on 400K data while using less than one-eighth of that amount (specifically, 3.6K CoT-PRM and 50K non-CoT PRM data).
- **A Novel and Effective Test-Time Scaling Approach.** Our VRPRM also serve as a highly effective test-time scaling strategy. It achieves significant performance improvements across multiple multimodal benchmarks, yielding a relative gain of up to 118% over the base model and substantially outperforming current state-of-the-art (SOTA) methods. This showcasing a new avenue for scaling model capabilities.

## 2 RELATED WORK

**Process Reward Models.** Process reward models (PRMs) are playing an increasingly critical role in reinforcement learning (RL) optimization and test time scaling (TTS). Unlike traditional Outcome Reward Models (ORMs) Whitehouse et al. (2025); Wang et al. (2025d;a); Zhang et al. (2024a), which assign a single score to the final output, PRMs evaluate each intermediate step in the generation process. These step-level signals are then aggregated into a final reward, providing more detailed supervision and reducing the issue of “spurious correctness,” where a model reaches the correct answer through flawed reasoning. This enables PRMs to show better generalization and stability in complex reasoning tasks. Qwen-Math-PRM Zhang et al. (2025b) combines Monte Carlo estimation with large language model judgments to filter and select a large set of process-level annotated data for supervised fine-tuning. VisualPRM Wang et al. (2025b) uses the InternVL2.5 model series to generate solution steps, applying Monte Carlo sampling to assess step-level accuracy. The model is trained by discretizing the output space into specific tokens. In summary, these studies mainly rely on process-level annotated data for fine-tuning foundation models, giving them process

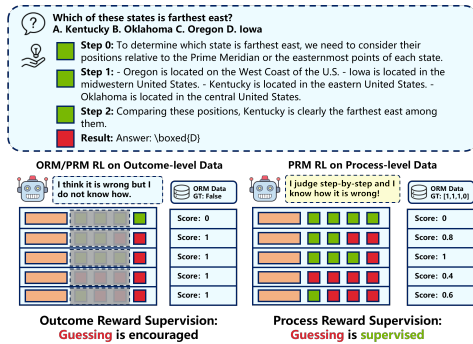


Figure 2: Process-level supervision provides a discriminative RL reward signal. However, under ORM-reward supervision, even when guessing at random, the model still maintains a 50% probability of being rewarded.

108 evaluation capabilities. However, these PRMs lack deep reasoning abilities and struggle to capture  
 109 the logical structures underlying complex reasoning paths.  
 110

111 **Chain-of-Thought Reward Models.** In recent years, research in reward modeling has shifted from  
 112 traditional scalar scoring models to Chain-of-Thought Reward Models (CoT-RMs), which generate  
 113 reasoning chains to assist in preference judgment. RRM Guo et al. (2025) treats reward modeling  
 114 as a reasoning task, using long-chain reasoning before generating the final reward, and introduces  
 115 a reinforcement learning (RL) framework to enhance reasoning ability. Many CoT-ORM studies  
 116 follow a two-stage training approach: first, supervised fine-tuning (SFT) for initialization, and then  
 117 RL to further improve performance. RM-R1 Chen et al. (2025a) and Think-RM Hong et al. (2025)  
 118 use high-quality long-chain reasoning data to guide the model via SFT and apply RL to improve  
 119 performance in the second stage. Later work extended CoT-ORM to multimodal settings. R1-  
 120 Reward Zhang et al. (2025a) uses GPT-4o to annotate a multimodal dataset and applies RL to en-  
 121 hance performance on complex reward tasks. UnifiedReward-Think Wang et al. (2025c) combines  
 122 multimodal preference data with RL to improve reasoning across text and images. The CoT ap-  
 123 proach is also used in Process Reward Models (PRMs), like GenPRM Zhao et al. (2025), which  
 124 uses explicit CoT reasoning and code verification but does not apply RL. CoT-enhanced reward  
 125 models improve interpretability and generalization, but they require high-quality CoT data, which is  
 126 costly to acquire and annotate.  
 127

### 128 3 METHODOLOGY

#### 129 3.1 PROBLEM FORMULATION

130 In this section, we introduce the preliminary setting of our research problem. Let  $\mathcal{D} = \{(I, P, S)\}$   
 131 denote a dataset consisting of a problem  $P$ , image  $I$ , and solution  $S$ . Each solution is composed of  
 132 multiple steps, denoted as  $S = (s_1, s_2, \dots, s_n)$ , where  $s_i$  represents the  $i$ -th step.  
 133

134 **Visual PRM.** In VisualPRM Wang et al. (2025b), in order to effectively utilize the generation capa-  
 135 bility of MLLM, the process evaluation is regarded as a multi-round dialogue, and the probability  
 136 value predicted by token 1 is used as the score of the step. Let  $M$  is a visual prm. Formally, the  
 137 output of the PRM can be represented as:

$$138 \quad y_i \sim M(1|I, P, s_{\leq i}), \quad (1)$$

139 where  $y_i$  denotes the score of  $i$ -th step. By setting a threshold to determine whether the step is  
 140 correct.

141 **Visual Reasoning PRM.** By equipping Visual PRM with an explicit reasoning process such as  
 142 CoT Wei et al. (2022), we have Visual Reasoning PRM. Before evaluating a step, we assume that  
 143 the model’s thinking about a problem  $P$ , image  $I$ , and solution  $S$  is  $\mathcal{T}$ , then the output of VRPRM  
 144 is,

$$145 \quad \mathcal{R} \sim \pi_\theta(I, P, (s_1, s_2, \dots, s_n), \mathcal{T}), \quad (2)$$

146 where  $\mathcal{T} \sim \pi_\theta(I, P, (s_1, s_2, \dots, s_n))$ , we extract the formatted output  $\mathcal{R}$  to obtain process reward  
 147  $(r_1, \dots, r_n)$ .  
 148

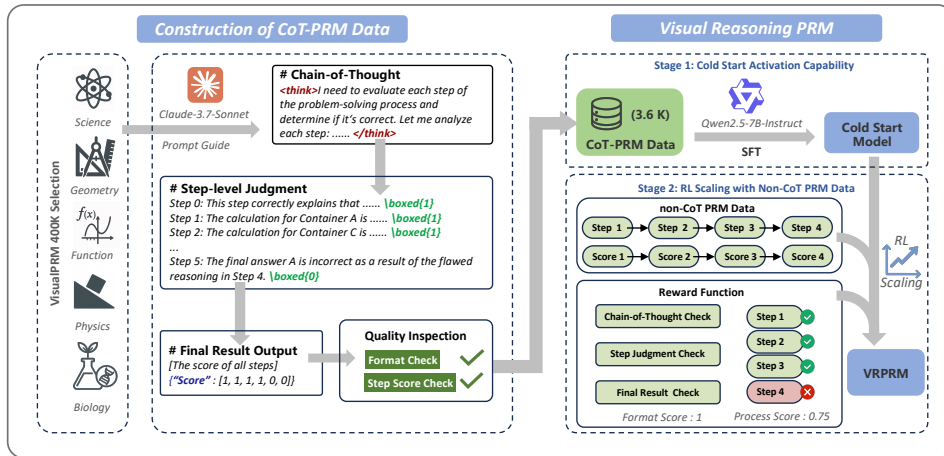
#### 149 3.2 COLD START ACTIVATION CAPABILITY

150 Although instruction-tuned LLMs have strong generalization capabilities and can complete basic  
 151 process evaluation tasks through prompts, these models often find it difficult to stably generate  
 152 structured and parsable evaluation results without cold start. Specifically, the model may not be able  
 153 to return evaluation results in the expected format, the process evaluation cannot be aligned with  
 154 the actual number of steps. Therefore, in this section, our main purpose is to stimulate the model  
 155 CoT and process evaluation capabilities. It mainly includes two parts: (1) synthesis of high-quality  
 156 CoT-PRM data and (2) SFT based on CoT-PRM data.  
 157

##### 158 3.2.1 SYNTHETIC COT-PRM DATA

159 VisualPRM400K Wang et al. (2025b) is a dataset of multimodal reasoning data with process la-  
 160 bel. We select data that is easy for the model to think and reason about, including science, ge-  
 161 ometry, functions, physics, biology and other fields. We select about 10K data, each of which

162  
163  
164  
165  
166  
167  
168  
169  
170  
171  
172  
173  
174  
175  
176



177  
178  
179  
180  
181  
182  
Figure 3: Overall framework of VRPRM. We first use Claude-3.7-Sonnet to generate CoT-PRM  
183 data with long-horizon reasoning on a small amount of VisualPRM400K data. **Two-stage training**  
184 **pipeline:** (1) **Cold Start:** We use CoT-PRM data to fine-tune the base model, helping it learn  
185 basic thinking and process evaluation capabilities. (2) **RL Scaling:** Then we use non-CoT PRM  
186 data to perform RL fine-tuning, further strengthening the model’s process evaluation and reasoning  
187 capabilities.

188 contains a prompt  $P$ , a step-by-step solution  $S = (s_1, \dots, s_n)$ , and a process-level annotation  
189  $G_r = (g_1, \dots, g_n)$ . Therefore, we can use a LLM to construct evaluation data with long-horizon  
190 reasoning and process-level annotations. In this study, we choose Claude-3.7-Sonnet as the data  
191 generator.

192 As shown in Fig 3, to ensure that the data is clearly structured and labeled consistently, we design  
193 a systematic prompting strategy that includes the following key steps: Step 1, we guide the model  
194 to conduct thinking part to fully understand the problem background, image information and the  
195 requirements of the evaluation task. The model’s thinking content needs to be placed between  
196  $\langle \text{think} \rangle$  and  $\langle / \text{think} \rangle$  tokens. Step 2, we then guide the model to perform a fine-grained analysis  
197 of each solution step and annotate the correctness of each step in a unified format, in the form of  
198  $\boxed{1}$  (correct) or  $\boxed{0}$  (incorrect). Step 3, the model must also return the intermediate  
199 results of the evaluation process in a standardized JSON format, such as  $\{\text{“Score”}:[r_1, \dots, r_n]\}$ ;

200 Based on the above process, we build a batch of PRM data with clear structure and complete long-  
201 horizon reasoning. For each generated sample, we implement a strict data quality inspection process  
202 to ensure the format specification and label consistency; all data that did not strictly follow the spec-  
203 ified format output or the evaluation results deviated from the reference label were eliminated. We  
204 finally obtained a dataset containing about 3.6K high-quality question-answer pairs, with a positive-  
205 negative sample ratio of about 1:1. For detailed prompt and statistics, please see the Appendix A.

### 206 3.2.2 SUPERVISED FINE TUNING

207 We use the above high-quality data to perform SFT on the target model to help the model master  
208 basic long-horizon reasoning and initial process assessment capabilities. Its training objectives are  
209 defined as follows:

$$r_\theta = \arg \min_{\theta} \mathbb{E}_{(I, P, S, C) \sim \mathcal{D}_{SFT}} [-\log P_\theta(C|I, P, S)], \quad (3)$$

210 Where  $\mathcal{D}_{SFT}$  is a constructed CoT-PRM dataset,  $P$  is the problem,  $S$  is the candidate solution, and  
211  $C$  is the target output, including the chain-of-thinking, step-level judgement, and final result output.

### 212 3.3 RL SCALING WITH NON-COT PRM DATA

213 To further enhance the model’s evaluation ability, we recommend reinforcement learning of the fine-  
214 tuned model  $r_\theta$  on step-level annotated data. We directly use the fine-tuned process reward model  
215  $r_\theta$  as the policy model for optimization, and its objective function is as follows:

$$\max_{r_\theta} \mathbb{E}_{(I, P, S, G_r) \sim \mathcal{D}_{prm}, O \sim r_\theta(I, P, S)} [\mathcal{R}(G_r, O)] - \beta \mathbb{D}_{KL}(r_\theta \| r_{\text{ref}}) \quad (4)$$

216 Where  $r_{ref}$  is the reference reward model. In practice, we use the checkpoint before RL training as  
 217  $r_{ref}$ , that is, the model checkpoint obtained after fine-tuning.  $I, P, S$  represents the image, problem,  
 218 and solution extracted from the data  $\mathcal{D}_{prm}$ ,  $G_r = (g_1, \dots, g_n)$  represents the step-level annotation  
 219 result, and  $O$  represents the text generated by the reward model, which includes the thought chain  
 220 and process judgment and result output.  $\mathcal{R}(G_r, O)$  is the reward function, and  $\mathbb{D}_{KL}$  is the KL  
 221 divergence. In practice, we use Group Relative Policy Optimization (GRPO) Shao et al. (2024) to  
 222 optimize the objective in the formula.

### 223 3.3.1 REWARD FUNCTION DESIGN

225 The rule-based reward mechanism has proven effective in enhancing the model’s reasoning ability.  
 226 In our approach, we design two reward rules when using step-level annotated data for RL: format  
 227 compliance and process accuracy.

228 First, the model output must follow a predefined format, which we regard as a reflection of the  
 229 model’s basic evaluation capabilities. Specifically, the model output should contain the following  
 230 structural elements: the `<think>...` `</think>` token for the thought chain, the `\boxed{0 or 1}` used  
 231 for step-by-step judgment, and the JSON format output of the final evaluation result, including  
 232 `{"Score": [...]}`. The existence of these tokens facilitates the structured extraction of the model’s  
 233 evaluation results. Therefore, if the model does not follow the format requirements, its format reward  
 234 will be set to zero:

$$235 \mathcal{R}_{format}(O) = \text{has\_think}(O) \wedge \text{has\_step\_judge}(O) \wedge \text{has\_final\_judge}(O) \quad (5)$$

236 Since this reward primarily prevents format violations, we assign it a lower weight, as our main focus  
 237 during the RL stage is improving the model’s evaluation capability rather than format adherence.

238 While format compliance reflects basic output skills, we further introduce process accuracy to eval-  
 239 uate each step of the model’s reasoning. This reward is based on the accuracy of the model’s predic-  
 240 tions for each step. If the final judgment is incorrect, the process reward is set to zero:

$$242 \mathcal{R}_{process}(G_r, O) = \begin{cases} 0, & \text{if } 1[g_o = r_o] = 0; \\ 243 \frac{1}{n} \sum_{i=1}^n 1[g_i = r_i], & \text{otherwise.} \end{cases} \quad (6)$$

245 Here,  $1[\cdot]$  is the indicator function,  $g_o$  is defined by the process annotation  $G_r$  (as in Eq 7), and  $r_o$  is  
 246 defined by the process reward extracted from  $O$ , similar to  $g_o$ .

$$248 g_o = \begin{cases} 0, & \text{if } 0 \in G_r; \\ 249 1, & \text{otherwise.} \end{cases} \quad (7)$$

250 The final reward function is,

$$251 \mathcal{R}(G_r, O) = w_f * \mathcal{R}_{format} + w_p * \mathcal{R}_{process} \quad (8)$$

252 Where  $w_f$  and  $w_p$  correspond to the weights of  $\mathcal{R}_{format}$  and  $\mathcal{R}_{process}$  respectively. In the work we  
 253 set  $w_f = 0.1$  and  $w_p = 0.9$ .

### 254 3.4 TEST-TIME SCALING

257 We follow VisualPRM’s setup for BoN Wang et al. (2025b), we set the critic model as a Process  
 258 Reward Model (PRM) to select the best response from multiple candidate responses.

259 In the inference phase, PRM scores the generation process of each response step by step: for a  
 260 response  $S = (s_1, s_2, \dots, s_n)$ , we let the PRM model predict the next token at each position and  
 261 use the probability of token “1” as the reward for that step. Formally, the reward score at each step  
 262 is defined as:

$$263 r_t = P_\theta(1|x, s_{<t}) \quad (9)$$

264 where  $x$  is the input prompt,  $s_{<t}$  represents the previous  $t - 1$  steps. For the  $N$  candidate responses  
 265  $\{S_1, S_2, \dots, S_N\}$  generated by the model, we input each candidate response into PRM for process  
 266 scoring and obtain the corresponding average score. Finally, the response with the highest score is  
 267 selected as the output through the following formula:

$$268 S = \arg \max_{S_i \in \{S_1, S_2, \dots, S_N\}} \frac{1}{n} \sum_{t=1}^n P_\theta(1|x, s_{<t}^i). \quad (10)$$

270  
 271 **Table 1: VisualProcessBench results reported with FEI and AEI.** **Bold** indicates the best result,  
 272 underlined indicates the second best result. w/o CoT means VRPRM does not perform explicit  
 273 reasoning, w/o RL means VRPRM does not perform RL training.

Model Name	# Samples	MMMU		MathVision		MathVerse-VO		DynaMath		WeMath		FEI Avg.	AEI Avg.
		FEI	AEI										
<b>Proprietary Models</b>													
GPT-4o-mini	unk	40.45	35.27	27.39	35.10	28.36	34.44	40.35	37.46	45.70	37.30	36.45	35.91
Gemini-2.0-Flash	unk	43.07	43.04	30.48	40.68	36.16	40.89	55.79	43.25	52.92	42.99	43.68	42.17
<b>Open-source Models</b>													
InternVL2.5-8B	unk	41.63	49.59	30.67	42.61	42.96	43.62	48.88	51.24	55.33	43.35	43.89	46.08
Qwen2.5-VL-7B	unk	44.57	46.88	36.94	39.54	46.69	42.75	52.81	52.89	60.82	44.76	48.37	45.36
Qwen2.5-VL-72B	unk	46.44	51.31	34.27	41.88	42.50	45.92	51.75	53.25	57.73	46.74	46.54	47.82
MiMo-VL-7B	unk	50.94	58.45	38.27	61.60	<b>48.71</b>	66.15	<b>60.50</b>	66.81	57.05	63.87	51.09	63.38
VisualPRM-8B	400K	30.71	59.01	24.58	62.91	24.56	60.93	30.00	62.08	18.21	60.22	25.61	61.03
<b>Ours</b>													
VRPRM	53.6K	52.06	63.16	42.98	67.34	40.94	63.80	53.51	67.95	59.11	67.76	49.72	66.00
- w/o CoT	53.6K	46.44	52.66	26.83	51.95	34.80	54.72	41.05	53.06	41.58	55.90	38.14	53.66
- w/o RL	3.6K	47.57	55.94	33.99	61.82	43.96	62.43	52.46	63.08	50.86	67.30	45.77	62.11
- w/o RL & w/o CoT	3.6K	49.06	50.69	33.15	54.57	41.72	51.70	50.18	55.26	48.80	48.79	44.58	52.20
VRPRM-MiMo	53.6K	53.18	<b>66.95</b>	<b>46.07</b>	<b>72.87</b>	47.95	<b>71.93</b>	59.47	<b>74.55</b>	<b>66.32</b>	78.26	<b>54.60</b>	<b>72.91</b>
- w/o CoT	53.6K	<u>54.31</u>	65.52	<u>43.40</u>	69.99	45.42	<u>71.05</u>	59.12	<u>73.20</u>	<u>62.89</u>	<b>78.34</b>	<u>53.03</u>	<u>71.62</u>
- w/o RL	3.6K	50.26	57.63	39.36	60.51	48.46	61.87	60.04	61.67	55.73	61.38	50.77	60.61
- w/o RL & w/o CoT	3.6K	<b>55.06</b>	45.35	35.81	44.24	46.69	46.55	59.65	50.48	60.82	47.22	51.61	46.77
VRPRM-Qwen3	53.6K	52.81	<u>65.78</u>	42.13	<u>70.48</u>	44.93	70.19	57.02	72.76	62.20	70.85	51.82	70.01
- w/o CoT	53.6K	46.44	62.34	39.89	70.15	38.99	67.23	53.33	71.85	57.04	71.57	47.14	68.63

## 4 EXPERIMENTS

In this section, we aim to answer the following questions:

- **Q1:** How does the performance of VRPRM compare to previous PRMs?
- **Q2:** How does VRPRM benefit policy model test-time scaling?
- **Q3:** Can VRPRM effectively exploit CoT reasoning to improve its performance?

### 4.1 EXPERIMENT SETTINGS

**Base Model.** We followed the setup of VisualPRM Wang et al. (2025b), selecting Qwen2.5-7B-Instruct, MiMo-VL-7B-SFT-2508 and Qwen3-4B-VL-Thinking as the initial base model. MiMo-VL-7B-SFT-2508 and Qwen3-4B-VL-Thinking are multimodal models with reasoning capabilities. We first performed SFT to give the model preliminary process scoring capabilities and obtained Cold Start Model. Then we performed RL training on it to strengthen the model capabilities and generate VRPRM, VRPRM-MiMo and VRPRM-Qwen3.

**Benchmarks.** We chose VisualProcessBench Wang et al. (2025b), a widely used multimodel process reward model evaluation benchmark. Each test example in the dataset contains a problem, a step-by-step solution, and a step-level label that reflects whether each step is correct or not. Following the setup of VisualPRM Wang et al. (2025b), we evaluate the best-of-N results of our VRPRM on five benchmarks: MathVista Lu et al. (2024), MathVision Wang et al. (2024), MathVerse Zhang et al. (2024b), WeMath Qiao et al. (2024), and LogicVista Xiao et al. (2024), which will be described in Appendix B.

**Training Settings.** In the SFT stage, for all base models the LoRA rank was set to 16 with an alpha value of 32, the learning rate was  $1.0e^{-4}$ , and the model was fine-tuned for 3 epochs. We set the per-device batch size to 1 and used 4 gradient accumulation steps. In the RL stage, we use verl Sheng et al. (2024) as our training framework. We train for 2 episodes using the AdamW optimizer with a learning rate of  $1.0e^{-6}$  and KL penalty with a coefficient of  $1.0e^{-6}$ . The RL training operated with a global batch size of 512. For Qwen2.5-VL-7B and MiMo-VL-7B-SFT-2508, we use four 80GB NVIDIA A800 GPUs for SFT and eight for RL. For Qwen3-4B-VL-Thinking, we use NVIDIA H200 GPUs with the same settings.

**Evaluation Metrics.** Inspired by Wang et al. (2025b); Zheng et al. (2024), we use the First Error Identification (FEI) and All Error Identification (AEI) to evaluate the performance of the PRM process evaluation. FEI requires the PRM to identify the first error encountered during reasoning. AEI assesses the PRM’s ability to identify all errors in a given solution. Both of them are calculated by F1 scores. This comprehensive error identification is crucial for providing fine-grained rewards during training, enabling effective reinforcement learning. We also record the computation overhead on MMMU benchmark as in table 2, including tokens per sample and processing time. The full computation overhead statistics on VisualProcessBench is in Appendix C.

## 4.2 VISUALPROCESSBENCH RESULTS

**Performance Analysis.** Table 1 shows the performance of the PRM model on VisualProcessBench, where **VRPRM significantly outperforms all existing methods, including both proprietary and open-source models**. Specifically, VRPRM-7B-MiMo and VRPRM-7B-Qwen lead across all sub-datasets. VRPRM-7B-MiMo achieves an average AEI of 66.44 and an average FEI of 51.54, outperforming the leading multimodal PRM, VisualPRM, by 5.41 in AEI and 25.93 in FEI. VRPRM-7B-Qwen also shows improvements of 4.97 in AEI and 24.11 in FEI, despite using only 13.4% of the training data. This highlights the effectiveness of our combined training scheme in boosting performance while keeping data requirements low. Notably, VRPRM without RL (VRPRM-7B-Qwen w/o RL and VRPRM-7B-MiMo w/o RL), trained on just 3.6K samples, achieved strong average AEIs of 62.11 and 60.61, outperforming all other open-source and proprietary models except MiMo-VL-7B. However, VRPRM-7B-MiMo w/o RL showed a slight performance drop compared to its base model, indicating that the initial SFT phase may have partially disrupted its CoT structure. Nevertheless, the subsequent RL training phase helped to recover this gap. See the Ablation Analysis for more details, and Appendix C for responses to VRPRM.

**Computational Overhead Analysis.** As shown in Table 2, the primary computational overhead stems directly from generating detailed reasoning process. For instance, VRPRM generates an average of 339.73 output tokens per sample compared to 10.03 tokens per sample for the non-reasoning baseline, resulting in an inference time increase from 0.39s to 16.94s per sample.

Table 2: **Computation overhead analysis on VisualProcessBench(MMMU)**. Metrics include average token counts and processing time per sample/reward.

Model	Total Tokens / Sample	Output Tokens / Sample	Input Tokens / Sample	Time / Sample (s)	Time / Reward (s)
VRPRM	2305.82	339.73	1966.08	16.94	1.5353
- w/o CoT	1976.12	10.03	1966.08	0.39	0.0385
VRPRM-MiMo	2994.63	1028.54	1966.08	20.40	1.8435
- w/o CoT	1976.12	10.03	1966.08	0.40	0.04
VRPRM-Qwen3	2410.66	584.34	1826.31	23.06	2.0815
- w/o CoT	1836.35	10.03	1826.31	0.30	0.0298
VisualPRM-8B	1344.88	10.03	1334.85	0.071	0.0071

## 4.3 BEST-OF-N EVALUATION RESULTS

We use VRPRM as the evaluation model for the BoN task with N set to 8. The InternVL2.5 Chen et al. (2025b) policy model generates N responses through a Chain of Thought (CoT) reasoning process with a temperature of 0.7. The highest-scoring response is selected as the final result. Some results are sourced from the OpenCompass leaderboard Buitrago & Nystrom (2019).

As shown in Table 3, VRPRM significantly improves performance on multiple multimodal reasoning benchmarks. When integrated into the InternVL2.5-8B model, VRPRM led to substantial improvements across all sub-datasets, achieving an overall relative improvement of up to 41.82% over the state-of-the-art VisualPRM. Using VRPRM as a critic model, the InternVL2.5-8B model, with fewer than 10B parameters, outperformed leading proprietary models such as GPT-4o, Claude-3.5, and Gemini-2.0-Flash in reasoning tasks. This demonstrates that test-time scaling can unlock

378 the latent reasoning potential of foundation models. Similar trends were observed for the larger  
 379 InternVL2.5-26B and InternVL2.5-38B models.  
 380

381 In summary, the open-source InternVL2.5 model, combined with VRPRM, outperforms proprietary  
 382 models across multiple tasks using the Best-of-8 strategy, especially in tasks requiring advanced  
 383 logical reasoning, such as MathVerse-VO and LogicVista. This confirms that VRPRM, trained using  
 384 our hybrid data method, significantly enhances process evaluation and cross-task transferability in  
 385 large multimodal models for complex tasks.  
 386

387 **Table 3: Best-of-8 Results on five multimodal reasoning benchmarks.** For MathVerse, we report  
 388 the performance on Vision-Only (VO) split. The overall score is the average score of the above  
 389 benchmarks.

390 <b>Model</b>	391 <b>MathVista</b>	392 <b>MathVision</b>	393 <b>MathVerse-VO</b>	394 <b>WeMath</b>	395 <b>LogicVista</b>	396 <b>Overall</b>
397 Proprietary Models						
398 GPT-4o	60.00	31.20	40.60	45.80	52.80	46.08
399 Gemini-2.0-Flash	70.40	43.60	47.80	47.40	52.30	52.30
400 Claude-3.5-Sonnet	65.30	35.60	46.30	44.00	60.40	50.32
401 Open-source Models						
402 InternVL2.5-8B	64.50	17.00	22.80	23.50	36.38	32.84
403 +VisualPRM	68.50	25.70	35.80	36.50	43.80	42.06
404 +4.00	+8.70	+13.00	+13.00	+7.80	+9.30	
405 +VRPRM w/o RL	72.60	33.95	39.85	44.29	64.43	51.02
406 +8.10	+16.95	+17.05	+20.79	+28.05	+18.19	
407 +VRPRM	79.10	51.44	51.52	36.71	79.46	59.65
408 +14.60	+34.44	+28.72	+13.21	+43.08	+27.23	
409 InternVL2.5-26B	68.20	23.40	24.00	30.90	39.64	37.23
410 +VisualPRM	73.10	29.60	39.10	40.80	51.00	46.72
411 +4.9	+6.20	+15.10	+9.90	+11.40	+9.50	
412 +VRPRM w/o RL	77.40	37.99	44.29	48.76	68.90	55.47
413 +9.20	+14.59	+20.29	+17.86	+29.26	+18.24	
414 +VRPRM	81.20	55.79	53.55	40.14	83.00	62.74
415 +13.00	+32.39	+29.55	+9.24	+43.36	+25.51	
416 InternVL2.5-38B	71.90	32.20	36.90	38.30	47.90	45.44
417 +VisualPRM	73.90	35.20	46.70	46.20	53.70	51.14
418 +2.00	+3.00	+9.80	+7.90	+5.80	+5.70	
419 +VRPRM w/o RL	78.40	43.45	51.52	51.43	70.02	58.96
420 +6.50	+11.25	+14.62	+13.13	+22.12	+13.52	
421 +VRPRM	83.50	59.41	58.76	46.86	84.78	66.66
422 +11.60	+27.21	+21.86	+8.56	+36.88	+21.22	

#### 414 4.4 ABLATION STUDIES

##### 415 4.4.1 EFFECTS OF BoN

416 In this experiment, to further verify the cross-model generalization ability of our method, we con-  
 417 ducted BoN experiments on four benchmark datasets: LogicVista, MathVerse-VO, MathVista, and  
 418 MathVision, using the InternVL2.5-8B and Qwen2.5-VL-7B models as policy models. We eval-  
 419 uated the following discriminative models: VRPRM w/o RL, VRPRM, VRPRM-Qwen3, and the  
 420 baseline models VisualPRM and MM-PRM.

421 As shown in Figure 4 and Figure 5, the inference accuracy of InternVL2.5-8B and Qwen2.5-VL-7B  
 422 steadily improved with the increase of the number of candidates N. VRPRM and VRPRM-Qwen3  
 423 both showed significant performance improvements, outperforming the MM-PRM baseline model  
 424 and the majority voting method (Major@K) on all datasets. Notably, the performance of MM-PRM  
 425 tends to plateau or improve slowly as N increases (e.g., on the LogicVista dataset), while the variant  
 426 of VRPRM maintains a strong upward trend, significantly narrowing the gap with the Pass@K upper  
 427 limit. Furthermore, the comparable performance of VRPRM and VRPRM-Qwen3 demonstrates that  
 428 our training paradigm is effective for different model architectures, including those with intrinsic  
 429 thinking capabilities.  
 430

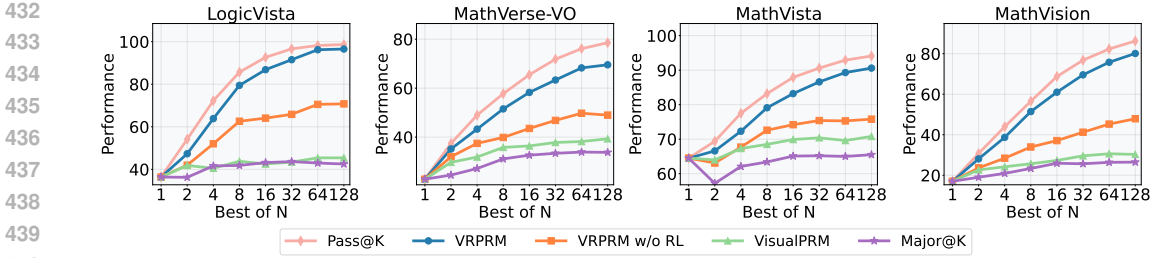


Figure 4: Best-of-N results of InternVL2.5-8B across four multimodel reasoning benchmarks using VisualPRM, VRPRM w/o RL, and VRPRM as critic models. The result of Pass@K is the upper bound.

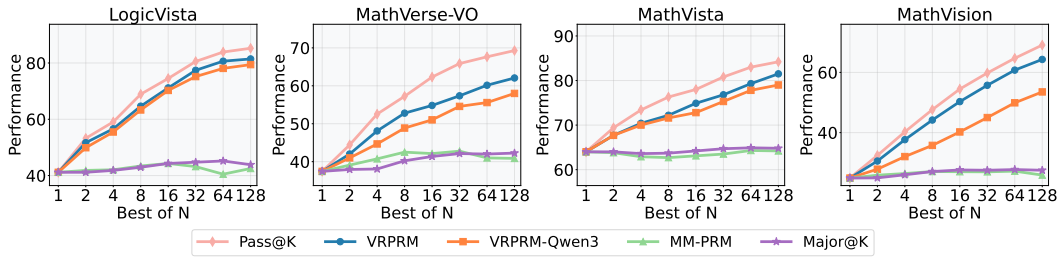


Figure 5: Best-of-N results of Qwen2.5-VL-7B across four multimodel reasoning benchmarks using VRPRM, VRPRM-Qwen3, and MM-PRM as critic models. The result of Pass@K is the upper bound.

#### 4.4.2 EFFECTS OF COT

In this experiment, we removed the model’s chain of thought reasoning module so that the model no longer performs explicit reasoning when evaluating multi-step solutions. This aims to observe whether VRPRM can effectively utilize CoT reasoning to improve its performance and to analyze the associated computational trade-offs.

**Performance Gain.** The results in Table 1 reveal that removing the CoT module leads to a significant degradation in evaluation performance across all metrics. For instance, for VRPRM-Qwen, the Average All Error Identification (AEI) drops sharply from 66.00 to 53.66, and the First Error Identification (FEI) declines from 49.72 to 38.14. A similar trend is observed in the model trained on MiMo and Qwen3, where the full VRPRM outperforms its non-reasoning counterpart. These results confirm that the model’s ability to perform fine-grained error correction is heavily dependent on the intermediate reasoning steps.

**Computational Overhead.** We acknowledge that this performance improvement comes at the cost of increased latency and token consumption. As detailed in Table 2, enabling CoT reasoning increases the average output tokens per sample from 10.03 to 339.73 for VRPRM, resulting in a corresponding increase in processing time from 0.39 to 16.94 seconds per sample. However, this overhead is a necessary trade-off. As illustrated above, the computation allocated to the reasoning process enables the model to perform fine-grained error identification. Also, unlike traditional reward models, VRPRM can provide transparent reasoning processes, transforming from a scorer to a white-box trustworthy verifier. An example output is provided in Appendix G.

In summary, while CoT reasoning introduces computational overhead, it is indispensable for enhancing reward modeling performance. It allows the model to better understand causal relationships and logic between steps, improving its ability to evaluate complex reasoning and make more accurate judgments. Without this capability, the model is more prone to misunderstand intermediate steps, leading to lower evaluation quality.

#### 4.4.3 EFFECTS OF RL

In this experiment, we investigated whether reinforcement learning (RL) could improve a model’s process evaluation capabilities. The performance of the VRPRM model without RL training (VR-

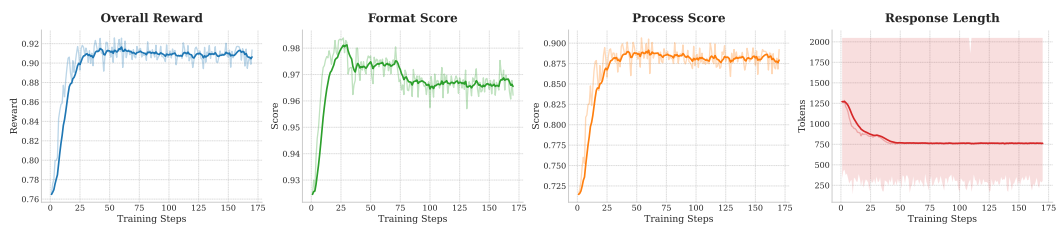
486 PRM w/o RL) is reported on the VisualProcessBench and BoN test sets in Tables 1 and 3, respectively.  
 487  
 488

489 On the VisualProcessBench, the VRPRM w/o RL, trained with CoT-PRM data during supervised  
 490 fine-tuning (SFT), outperformed VisualPRM, the state-of-the-art multimodal PRM, in both average  
 491 FEI and AEI. We then applied RL training to the VRPRM w/o RL using PRM data, creating the com-  
 492 plete VRPRM model. This resulted in a 3.92% average performance improvement on VisualPro-  
 493 cessBench, with gains across all sub-datasets. In the BoN test, VRPRM consistently outperformed  
 494 VRPRM without RL across various InternVL model scales, with a maximum relative improvement  
 495 of 9.04%.

496 These results show that RL training based on non-CoT PRM data significantly enhances process  
 497 evaluation capabilities. By incorporating RL, we can effectively train a PRM model with improved  
 498 evaluation skills at a relatively low data cost.

#### 499 4.4.4 RL TRAINING DYNAMICS

500 To verify the stability of our reinforcement learning process, we visualize the training trajectories  
 501 of VRPRM in Figure 6. The curves track the Overall Reward, Format Score, Process Score, and  
 502 Response Length across training steps. As illustrated, the Overall Reward exhibits a consistent up-  
 503 ward trend before converging to a stable plateau, indicating that the model effectively optimizes  
 504 the objective function via GRPO without experiencing significant crashes or spikes. This confirms  
 505 the robustness of our RL formulation. Notably, the Response Length begins at a higher value but  
 506 gradually decreases and stabilizes during training. This suggests that the model learns to gener-  
 507 ate more efficient and concise reasoning paths rather than exploiting length-based reward hacking.  
 508 Collectively, these dynamics demonstrate a healthy and stable training process.



510  
 511 Figure 6: VRPRM training curves. Evolution of reward metrics (Overall, Format, Process) and  
 512 513 average response length during the RL fine-tuning stage.  
 514  
 515  
 516

## 520 5 CONCLUSION

521 In this paper, we introduce VRPRM, the first Visual Reasoning Process Reward Model capable of  
 522 incorporating RL reasoning. We have designed a two-stage training strategy for this model. The first  
 523 stage involves supervised fine-tuning (SFT) on a small set of high-quality CoT data to “activate” the  
 524 model’s reasoning potential. This is followed by a second stage of “reinforcement” through rein-  
 525 forcement learning (RL) using a large volume of lower-cost non-CoT data. Our approach addresses  
 526 the common deficiency in deep reasoning abilities found in existing process reward models and  
 527 mitigates the prohibitively high data annotation costs associated with introducing CoT capabilities.

528  
 529 Experimental results demonstrate that VRPRM comprehensively outperforms non-thinking visual  
 530 process reward models trained on 400K data instances, while using only one-eighth of the training  
 531 data. This proves the exceptional data efficiency of our method. Furthermore, VRPRM exhibits  
 532 outstanding test-time scaling capabilities, achieving up to a 118% relative performance improvement  
 533 on multiple multimodal reasoning benchmarks. This demonstrates that VRPRM is also an effective  
 534 test-time scaling strategy.

535 In conclusion, VRPRM offers a novel training paradigm for the future development of process re-  
 536 ward models, which can significantly enhance the model’s complex reasoning and evaluation ca-  
 537 pabilities while substantially reducing annotation costs. We believe that this data-efficient training  
 538 strategy not only carves out a new path for multimodal reward modeling but also provides valuable  
 539 insights for building more powerful and generalizable reward models in a broader range of fields in  
 the future.

540 

## 6 ETHICS STATEMENT

541  
542 We acknowledge the ICLR Code of Ethics and affirm that our work complies with its principles. Our  
543 research does not raise any immediate ethical concerns. We have considered the potential broader  
544 impacts of our work, and we detail our considerations below.545 About data usage and privacy, the datasets used in this study are publicly available and were collected  
546 in accordance with their original licenses. Our work does not involve the collection of personal data.  
547 We have adhered to best practices in data anonymization and privacy preservation where applicable.548 About potential biases and fairness, the methods proposed in this work has little risk on introducing  
549 biases and unfairness. We have taken steps to mitigate such risks. We encourage further scrutiny  
550 and responsible use of our methodology.551 About social impact, we believe our research contributes positively. We do not foresee our work  
552 being used for malicious purposes, but we acknowledge that any technology can be misused. We  
553 encourage the community to use our work responsibly.554 About human subjects, this study did not involve human subjects, and no ethical approval was  
555 required.

556 About conflicts of interest: The authors declare no conflicts of interest.

559 

## 560 7 REPRODUCIBILITY STATEMENT

561 To facilitate the reproducibility of our work, we have made the following efforts:

562 About availability, we provide a complete, anonymized implementation of our proposed VRPRM  
563 framework, including training and evaluation scripts, as supplementary material. The code will be  
564 made publicly available upon publication. The code, models and datasets used in our work are  
565 almost all open source and can be easily accessed from the internet.566 About experimental setup, our experimental setup is comprehensively documented in the experiment  
567 section and appendix to allow for exact replication of our results.570 

## 571 REFERENCES

572 Paola A. Buitrago and Nicholas A. Nystrom. Open compass: Accelerating the adoption of ai in  
573 open research. In *Practice and Experience in Advanced Research Computing 2019: Rise of  
574 the Machines (Learning)*, PEARC ’19, New York, NY, USA, 2019. Association for Computing  
575 Machinery. ISBN 9781450372275. doi: 10.1145/3332186.3332253. URL <https://doi.org/10.1145/3332186.3332253>.577 Xiusi Chen, Gaotang Li, Ziqi Wang, Bowen Jin, Cheng Qian, Yu Wang, Hongru Wang, Yu Zhang,  
578 Denghui Zhang, Tong Zhang, et al. Rm-r1: Reward modeling as reasoning. *arXiv preprint  
579 arXiv:2505.02387*, 2025a.581 Zhe Chen, Weiyun Wang, Yue Cao, Yangzhou Liu, Zhangwei Gao, Erfei Cui, Jinguo Zhu, Shen-  
582 glong Ye, Hao Tian, Zhaoyang Liu, Lixin Gu, Xuehui Wang, Qingyun Li, Yimin Ren, Zixuan  
583 Chen, Jiapeng Luo, Jiahao Wang, Tan Jiang, Bo Wang, Conghui He, Botian Shi, Xingcheng  
584 Zhang, Han Lv, Yi Wang, Wenqi Shao, Pei Chu, Zhongying Tu, Tong He, Zhiyong Wu, Huipeng  
585 Deng, Jiaye Ge, Kai Chen, Kaipeng Zhang, Limin Wang, Min Dou, Lewei Lu, Xizhou Zhu,  
586 Tong Lu, Dahua Lin, Yu Qiao, Jifeng Dai, and Wenhui Wang. Expanding performance bound-  
587 aries of open-source multimodal models with model, data, and test-time scaling, 2025b. URL  
588 <https://arxiv.org/abs/2412.05271>.589 Tianzhe Chu, Yuexiang Zhai, Jihan Yang, Shengbang Tong, Saining Xie, Dale Schuurmans, Quoc V  
590 Le, Sergey Levine, and Yi Ma. Sft memorizes, rl generalizes: A comparative study of foundation  
591 model post-training. *arXiv preprint arXiv:2501.17161*, 2025.592 Jiaxin Guo, Zewen Chi, Li Dong, Qingxiu Dong, Xun Wu, Shaohan Huang, and Furu Wei. Reward  
593 reasoning model. *arXiv preprint arXiv:2505.14674*, 2025.

594 Ilgee Hong, Changlong Yu, Liang Qiu, Weixiang Yan, Zhenghao Xu, Haoming Jiang, Qingru Zhang,  
 595 Qin Lu, Xin Liu, Chao Zhang, et al. Think-rm: Enabling long-horizon reasoning in generative  
 596 reward models. *arXiv preprint arXiv:2505.16265*, 2025.

597

598 Pan Lu, Hritik Bansal, Tony Xia, Jiacheng Liu, Chunyuan Li, Hannaneh Hajishirzi, Hao Cheng, Kai-  
 599 Wei Chang, Michel Galley, and Jianfeng Gao. Mathvista: Evaluating mathematical reasoning of  
 600 foundation models in visual contexts. In *International Conference on Learning Representations*  
 601 (*ICLR*), 2024.

602

603 Runqi Qiao, Qiuna Tan, Guanting Dong, Minhui Wu, Chong Sun, Xiaoshuai Song, Zhuoma  
 604 GongQue, Shanglin Lei, Zhe Wei, MiaoXuan Zhang, et al. We-math: Does your large multi-  
 605 modal model achieve human-like mathematical reasoning? *arXiv preprint arXiv:2407.01284*,  
 606 2024.

607

608 Zhihong Shao, Peiyi Wang, Qihao Zhu, Runxin Xu, Junxiao Song, Xiao Bi, Haowei Zhang,  
 609 Mingchuan Zhang, YK Li, Y Wu, et al. Deepseekmath: Pushing the limits of mathematical  
 610 reasoning in open language models. *arXiv preprint arXiv:2402.03300*, 2024.

611

612 Guangming Sheng, Chi Zhang, Zilingfeng Ye, Xibin Wu, Wang Zhang, Ru Zhang, Yanghua Peng,  
 613 Haibin Lin, and Chuan Wu. Hybridflow: A flexible and efficient rlhf framework. *arXiv preprint*  
 614 *arXiv: 2409.19256*, 2024.

615

616 Binghai Wang, Runji Lin, Keming Lu, Le Yu, Zhenru Zhang, Fei Huang, Chujie Zheng, Kai Dang,  
 617 Yang Fan, Xingzhang Ren, et al. Worldpm: Scaling human preference modeling. *arXiv preprint*  
 618 *arXiv:2505.10527*, 2025a.

619

620 Ke Wang, Junting Pan, Weikang Shi, Zimu Lu, Houxing Ren, Aojun Zhou, Mingjie Zhan, and  
 621 Hongsheng Li. Measuring multimodal mathematical reasoning with math-vision dataset. In *The*  
 622 *Thirty-eight Conference on Neural Information Processing Systems Datasets and Benchmarks*  
 623 *Track*, 2024. URL <https://openreview.net/forum?id=QWTCCxMpPA>.

624

625 Weiyun Wang, Zhangwei Gao, Lianjie Chen, Zhe Chen, Jinguo Zhu, Xiangyu Zhao, Yangzhou Liu,  
 626 Yue Cao, Shenglong Ye, Xizhou Zhu, et al. Visualprm: An effective process reward model for  
 627 multimodal reasoning. *arXiv preprint arXiv:2503.10291*, 2025b.

628

629 Yibin Wang, Zhimin Li, Yuhang Zang, Chunyu Wang, Qinglin Lu, Cheng Jin, and Jiaqi Wang.  
 630 Unified multimodal chain-of-thought reward model through reinforcement fine-tuning. *arXiv*  
 631 *preprint arXiv:2505.03318*, 2025c.

632

633 Yibin Wang, Yuhang Zang, Hao Li, Cheng Jin, and Jiaqi Wang. Unified reward model for multi-  
 634 modal understanding and generation. *arXiv preprint arXiv:2503.05236*, 2025d.

635

636 Jason Wei, Xuezhi Wang, Dale Schuurmans, Maarten Bosma, Fei Xia, Ed Chi, Quoc V Le, Denny  
 637 Zhou, et al. Chain-of-thought prompting elicits reasoning in large language models. *Advances in*  
 638 *neural information processing systems*, 35:24824–24837, 2022.

639

640 Chenxi Whitehouse, Tianlu Wang, Ping Yu, Xian Li, Jason Weston, Ilia Kulikov, and Swarnadeep  
 641 Saha. J1: Incentivizing thinking in llm-as-a-judge via reinforcement learning. *arXiv preprint*  
 642 *arXiv:2505.10320*, 2025.

643

644 Yijia Xiao, Edward Sun, Tianyu Liu, and Wei Wang. Logicvista: Multimodal llm logical reasoning  
 645 benchmark in visual contexts, 2024. URL <https://arxiv.org/abs/2407.04973>.

646

647 Lunjun Zhang, Arian Hosseini, Hritik Bansal, Mehran Kazemi, Aviral Kumar, and Rishabh  
 648 Agarwal. Generative verifiers: Reward modeling as next-token prediction. *arXiv preprint*  
 649 *arXiv:2408.15240*, 2024a.

650

651 Renrui Zhang, Dongzhi Jiang, Yichi Zhang, Haokun Lin, Ziyu Guo, Pengshuo Qiu, Aojun Zhou,  
 652 Pan Lu, Kai-Wei Chang, Yu Qiao, et al. Mathverse: Does your multi-modal llm truly see the  
 653 diagrams in visual math problems? In *European Conference on Computer Vision*, pp. 169–186.  
 654 Springer, 2024b.

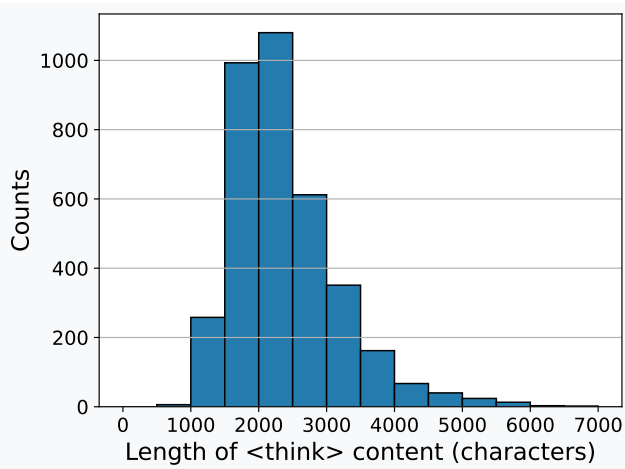
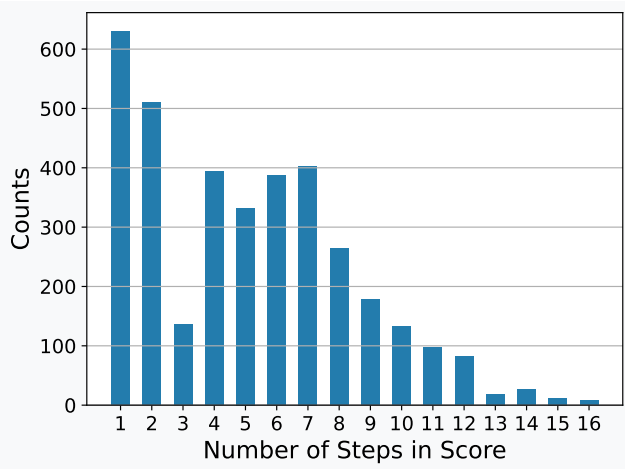
648 Yi-Fan Zhang, Xingyu Lu, Xiao Hu, Chaoyou Fu, Bin Wen, Tianke Zhang, Changyi Liu, Kaiyu  
649 Jiang, Kaibing Chen, Kaiyu Tang, et al. R1-reward: Training multimodal reward model through  
650 stable reinforcement learning. *arXiv preprint arXiv:2505.02835*, 2025a.

651  
652 Zhenru Zhang, Chujie Zheng, Yangzhen Wu, Beichen Zhang, Runji Lin, Bowen Yu, Dayiheng Liu,  
653 Jingren Zhou, and Junyang Lin. The lessons of developing process reward models in mathematical  
654 reasoning. *arXiv preprint arXiv:2501.07301*, 2025b.

655 Jian Zhao, Runze Liu, Kaiyan Zhang, Zhimu Zhou, Junqi Gao, Dong Li, Jiafei Lyu, Zhouyi Qian,  
656 Biqing Qi, Xiu Li, et al. Genprm: Scaling test-time compute of process reward models via  
657 generative reasoning. *arXiv preprint arXiv:2504.00891*, 2025.

658 Chujie Zheng, Zhenru Zhang, Beichen Zhang, Runji Lin, Keming Lu, Bowen Yu, Dayiheng Liu,  
659 Jingren Zhou, and Junyang Lin. Processbench: Identifying process errors in mathematical rea-  
660 soning. *arXiv preprint arXiv:2412.06559*, 2024.

661  
662  
663  
664  
665  
666  
667  
668  
669  
670  
671  
672  
673  
674  
675  
676  
677  
678  
679  
680  
681  
682  
683  
684  
685  
686  
687  
688  
689  
690  
691  
692  
693  
694  
695  
696  
697  
698  
699  
700  
701

702 A ROLLOUT PROMPT AND DATA STATISTICS  
703704 In this section we give a Prompt for synthetic data and an example of synthetic data. The prompt for  
705 using Claude-3.7-Sonnet to synthetic CoT-PRM Data is shown in Fig 9. The example of CoT-PRM  
706 Data is shown in Fig 10.707 We report the statistics of CoT-PRM Data. As shown in Fig 7, in CoT-PRM Data, more than 90%  
708 of the responses have a thought length of more than 1500 characters, which shows that CoT-PRM  
709 Data has good response quality and is a high-quality long-range reasoning process label dataset.  
710711 The step distribution statistics of CoT-PRM Data are shown in Fig 8. We observe that most solutions  
712 consist of fewer than 15 steps. Among these solutions with fewer than 15 steps, the number of steps  
713 has a sample distribution.730 Figure 7: Distribution of think Content Length  
731748 Figure 8: Distribution of Step Count  
749

## Prompt for Synthetic CoT-PRM Data

756  
757 [User]:  
758

759 You are a reasoning evaluator. Your task is to analyze problem-solving steps one by one. At  
760 the same time, according to the analysis process, judge whether the entire problem-solving  
761 is correct.

762  
763 For each solution step, you need to evaluate:  
764

765 Score (0 or +1):  
766

- \* +1: Completely correct reasoning
- \* 0: Completely incorrect
- \* Use two integers to determine whether the step is correct

767  
768 For the entire problem-solving, you need to evaluate:  
769

- \* +1: Completely correct reasoning
- \* 0: Completely incorrect

770 Requirements:  
771

- Analysis each step independently and provide scores as integer numbers. After analyzing each step, the analysis results of each step are given in the form of \boxed{Score}
- Evaluate the entire problem-solving and determine whether it is correct
- The scores of the evaluation steps are returned in strict JSON format: "Score": [scores], Ensure arrays have the same length with the number of solution steps
- Consider logical accuracy, mathematical coherence, and solution efficiency

772  
773 Example output format:  
774

775 <Step judgment >  
776 Analysis of each step, \boxed{1}  
777 <The score of all steps >  
778 {"Score": [1, 1, 0]}

779  
780 Question:  
781

782 {question}  
783

784 Answer:  
785

786 {answer}  
787

788  
789 You will gradually receive each step:  
790

791 [User]:  
792

793 Step {i}: {the i-th step}

Figure 9: Prompt for Synthetic CoT-PRM Data

## B MULTIMODAL REASONING BENCHMARKS

We selected five multimodal reasoning benchmarks:

**MathVista Lu et al. (2024)** is a benchmark specifically designed to evaluate the capabilities of Multimodal Large Language Models (MLLMs) in visual mathematical reasoning. The dataset contains 6,141 examples, sourced from 28 existing multimodal math-related datasets, along with three newly created subsets: IQTest, FunctionQA, and PaperQA. MathVista covers a wide range of tasks, including image interpretation, chart reasoning, geometry problem solving, and function graph analysis, aiming to assess models' abilities in processing complex visual information and performing compositional mathematical reasoning. We selected its mini test set, about 1000 samples.

**MathVision Wang et al. (2024)** is a meticulously constructed high-quality benchmark dataset designed to evaluate the visual mathematical reasoning abilities of MLLMs. The dataset contains 3,040

810  
811**An example of CoT-PRM Data**

812

**<think >**813  
814

I need to evaluate each step of the problem-solving process and determine if it's correct. Let me analyze each step:

815  
816  
817

Step 0: This step correctly explains that we need to consider the temperature difference between the liquid and room temperature, and that dew forms on cold surfaces. This is a good setup of the problem.

818

Step 1: Container A calculation:- Liquid temperature:  $36^{\circ}\text{C}$  - Room temperature:  $25^{\circ}\text{C}$  - Temperature difference:  $36^{\circ}\text{C} - 25^{\circ}\text{C} = 11^{\circ}\text{C}$ . This calculation is mathematically correct.

819

Step 2: Container B calculation: - Liquid temperature:  $63^{\circ}\text{C}$  - Room temperature:  $25^{\circ}\text{C}$  - Temperature difference:  $63^{\circ}\text{C} - 25^{\circ}\text{C} = 38^{\circ}\text{C}$ . This calculation is mathematically correct.

820

Step 3: Container C calculation: - Liquid temperature:  $83^{\circ}\text{C}$  - Room temperature:  $25^{\circ}\text{C}$  - Temperature difference:  $83^{\circ}\text{C} - 25^{\circ}\text{C} = 58^{\circ}\text{C}$ . This calculation is mathematically correct.

821

Step 4: This is where the reasoning error occurs. The step claims that Container A will form dew first because it has the smallest temperature difference. However, this is incorrect. Dew (water droplets) forms on surfaces that are COLDER than the surrounding air, not warmer. All containers have liquids that are warmer than room temperature ( $25^{\circ}\text{C}$ ).

822

For dew to form on the inner walls of the containers, the inner wall temperature would need to be below the dew point of the air inside the container. Since all liquids are warmer than room temperature, they will be warming the air inside their containers, not cooling it. When warm, humid air comes in contact with a cold surface, condensation occurs.

823

Therefore, Container C should show droplets first because it has the highest temperature difference, which creates the greatest potential for condensation when the warm, humid air inside contacts the relatively cooler walls.

824

Step 5: The final answer A is incorrect based on the faulty reasoning in Step 4.

825

So: - Steps 0-3: Correct (+1 each) - Step 4: Incorrect (0) - Step 5: Incorrect (0) since it's based on the incorrect reasoning from Step 4

826

The entire problem-solving process is incorrect because the core reasoning about how condensation forms is flawed.

827

**</think >**

828

**<Step judgment >**

829

Step 0: This step correctly explains that droplet formation involves temperature differences between the liquid and room temperature. However, there's a fundamental misunderstanding about when condensation occurs. Dew forms when warm, moist air contacts a surface that's cooler than the dew point temperature. \boxed{1}

830

Step 1: The calculation for Container A is mathematically correct ( $36^{\circ}\text{C} - 25^{\circ}\text{C} = 11^{\circ}\text{C}$ ). But simply calculating the temperature difference doesn't determine which container will form droplets first. \boxed{1}

831

Step 2: The calculation for Container B is mathematically correct ( $63^{\circ}\text{C} - 25^{\circ}\text{C} = 38^{\circ}\text{C}$ ). Again, simply calculating the difference is not incorrect, but the application of this will be important. \boxed{1}

832

Step 3: The calculation for Container C is mathematically correct ( $83^{\circ}\text{C} - 25^{\circ}\text{C} = 58^{\circ}\text{C}$ ). The mathematical operation is performed correctly. \boxed{1}

833

Step 4: This step contains the critical error. The reasoning incorrectly concludes that the container with the smallest temperature difference (Container A) will form dew first. In reality, when hot liquid is placed in a container at room temperature, the warmer liquid creates water vapor. The container with the highest temperature (Container C) will produce the most vapor, which will condense on the relatively cooler inner walls of the container (which are closer to room temperature). The larger the temperature difference, the more pronounced this effect will be. \boxed{0}

834

Step 5: The final answer A is incorrect as a result of the flawed reasoning in Step 4. Container C (the hottest) would be expected to show condensation first due to the greatest temperature differential producing the most water vapor. \boxed{0}

835

**<The score of all steps >**

836

```
{"Score": [1, 1, 1, 1, 0, 0]}
```

837

838

839

Figure 10: An Example of CoT-PRM Data

864 mathematical problems, all sourced from real-world math competitions. It spans 16 distinct mathematical disciplines and is categorized into 5 levels of difficulty, offering a comprehensive assessment across a wide range of topics and complexities. Its complete test set has about 3,000 samples.  
 865  
 866  
 867

868 **MathVerse Zhang et al. (2024b)** is a comprehensive visual math benchmark designed to provide fair and in-depth evaluation of mathematical diagram understanding and reasoning abilities in MLLMs. The dataset consists of 2,612 high-quality, multi-subject math problems with accompanying diagrams. Each problem is manually transformed into six distinct multimodal versions, varying in the degree of visual and textual information provided, resulting in a total of approximately 871 15,000 test samples. This design enables MathVerse to rigorously assess whether, and to what extent, MLLMs truly rely on visual diagrams for mathematical reasoning. We report the performance 872 on the Vision-Only split.  
 873  
 874

875 **WeMath Qiao et al. (2024)** is the first benchmark specifically designed to explore the underlying 876 problem-solving mechanisms of Multimodal Large Language Models (MLLMs) in visual mathematical 877 reasoning. Rather than focusing solely on final answer accuracy, We-Math emphasizes 878 how models apply knowledge during the reasoning process. The dataset consists of 6,500 carefully 879 curated visual math problems, covering 67 hierarchical knowledge concepts across 5 levels of 880 knowledge granularity, forming a structured and comprehensive knowledge evaluation framework.  
 881 We report "Score (Strict)" as the main indicator on its mini-test set of about 1740 samples.  
 882  
 883

884 **LogicVista Xiao et al. (2024)** is a benchmark specifically designed to evaluate the fundamental 885 logical reasoning abilities of Multimodal Large Language Models (MLLMs) within visual contexts.  
 886 It focuses on five core categories of logical reasoning tasks: spatial reasoning, deductive reasoning,  
 887 inductive reasoning, numerical reasoning, and mechanical reasoning, offering a comprehensive 888 assessment across key dimensions of logic. The dataset comprises 448 multiple-choice visual questions  
 889 drawn from diverse sources and question types, aiming to systematically assess the strengths and 890 limitations of current MLLMs in solving visual logic problems.  
 891  
 892

## 890 C MORE RESULTS ON COMPUTATION OVERHEAD 891

892 In Table 4, we give detailed token and time results of VRPRM, VRPRM-MiMo, VRPRM-Qwen3  
 893 and VisualPRM across VisualProcessBench.  
 894

## 895 D MORE ABLATION RESULTS 896

897 In Table 5, we give detailed Best-of-N results on InternVL2.5-8B across four multimodel reasoning  
 898 benchmarks using VisualPRM, VRPRM w/o RL, and VRPRM as a critic model. The Pass@K  
 899 results are provided as an upper bound, and the Major@K results are provided as a voting baseline.  
 900

## 901 E CROSS-MODEL GENERALIZATION RESULTS 902

904 In Table 6, we give detailed Best-of-N results on Qwen2.5VL-7B across four multimodel reasoning  
 905 benchmarks using MM-PRM, VRPRM, VRPRM-Qwen3 as a critic model. The Pass@K results are  
 906 provided as an upper bound, and the Major@K results are provided as a voting baseline.  
 907

908 The results presented in Table 6 demonstrate that our VRPRM training methodology effectively  
 909 generalizes to different policy models and base architectures, including reasoning model **Qwen3-**  
 910 **VL-4B-Thinking** (referred to as VRPRM-Qwen3). Consistent with the findings on the InternVL2.5  
 911 policy, the experiments on the Qwen2.5-VL-7B policy show that inference accuracy improves sig-  
 912 nificantly with an increasing number of response candidates  $N$ , while the performance gap between  
 913 our VRPRM critics and the baselines also widens, approaching the upper bound Pass@K results.  
 914

915 Taking **LogicVista** as a prime example, both VRPRM and VRPRM-Qwen3 exhibit superior per-  
 916 formance. At  $N = 128$ , VRPRM achieves an accuracy of 81.43, and VRPRM-Qwen3 reaches 79.42.  
 917 These scores not only substantially outperform the MM-PRM critic (42.51) and the Major@K vot-  
 918 ing baseline (43.85) by over 35 points but also closely approach the theoretical upper bound of  
 919 Pass@K (85.23). Similar trends are observed across the other benchmarks, such as MathVerse-VO  
 920 and MathVision, where our methods consistently dominate the baselines.  
 921

918

919

920

921

922

923

924

925

926

927

928

929

930

931

932

933

934

935

936

937

938

939

940

941

942

943

944

945

946

947

948

949

950

951

952

953

954

955

956

957

958

959

960

961

962

963

964

965

966

967

968

969

970

971

MMMU Statistics					
Model	Total Tokens / Sample	Output Tokens / Sample	Input Tokens / Sample	Time / Sample (s)	Time / Reward (s)
VRPRM	2305.82	339.73	1966.08	16.94	1.5353
- w/o CoT	1976.12	10.03	1966.08	0.39	0.0385
VRPRM-MiMo	2994.63	1028.54	1966.08	20.40	1.8435
- w/o CoT	1976.12	10.03	1966.08	0.40	0.04
VRPRM-Qwen3	2410.66	584.34	1826.31	23.06	2.0815
- w/o CoT	1836.35	10.03	1826.31	0.30	0.0298
VisualPRM-8B	1344.88	10.03	1334.85	0.071	0.0071
MathVision Statistics					
Model	Total Tokens / Sample	Output Tokens / Sample	Input Tokens / Sample	Time / Sample (s)	Time / Reward (s)
VRPRM	2464.82	354.12	2110.70	23.75	2.1871
- w/o CoT	2120.53	9.83	2110.70	0.31	0.0314
VRPRM-MiMo	3587.11	1476.41	2110.70	37.85	3.4944
- w/o CoT	2120.53	9.83	2110.70	0.33	0.0336
VRPRM-Qwen3	2537.94	580.52	1957.42	21.78	2.0082
- w/o CoT	1967.25	9.83	1957.42	0.23	0.0230
VisualPRM-8B	1480.39	9.83	1470.56	0.0829	0.0084
MathVerse Statistics					
Model	Total Tokens / Sample	Output Tokens / Sample	Input Tokens / Sample	Time / Sample (s)	Time / Reward (s)
VRPRM	3466.49	333.78	3132.71	24.44	2.3435
- w/o CoT	3412.14	9.42	3132.71	0.25	0.0268
VRPRM-MiMo	4434.05	1301.33	3132.71	38.22	3.6670
- w/o CoT	3142.14	9.42	3132.71	0.31	0.0331
VRPRM-Qwen3	3211.13	518.60	2692.53	22.20	2.1290
- w/o CoT	2701.95	9.42	2692.53	0.22	0.0229
VisualPRM-8B	1185.09	9.42	1175.67	0.0646	0.0069
DynaMath Statistics					
Model	Total Tokens / Sample	Output Tokens / Sample	Input Tokens / Sample	Time / Sample (s)	Time / Reward (s)
VRPRM	1900.15	312.95	1587.20	22.28	2.2683
- w/o CoT	1596.02	8.82	1587.20	0.21	0.0240
VRPRM-MiMo	2766.17	1178.97	1587.20	27.57	2.8012
- w/o CoT	1596.02	8.82	1587.20	0.27	0.0301
VRPRM-Qwen3	1975.85	506.21	1469.63	21.22	2.1614
- w/o CoT	1478.45	8.82	1469.63	0.20	0.0225
VisualPRM-8B	2773.59	8.82	2764.78	0.1447	0.0164
Wemath Statistics					
Model	Total Tokens / Sample	Output Tokens / Sample	Input Tokens / Sample	Time / Sample (s)	Time / Reward (s)
VRPRM	1782.72	334.48	1448.24	21.77	2.2080
- w/o CoT	1457.10	8.86	1448.24	0.25	0.0285
VRPRM-MiMo	2636.96	1188.71	1448.24	26.12	2.6492
- w/o CoT	1457.10	8.86	1448.24	0.23	0.0257
VRPRM-Qwen3	1880.29	498.62	1381.67	21.32	2.1592
- w/o CoT	1390.53	8.86	1381.67	0.22	0.0246
VisualPRM-8B	2582.33	8.86	2573.47	0.1352	0.0153

Table 4: **Computation overhead analysis on VisualProcessBench.** Metrics include average token counts and processing time per sample/reward.

972 These findings highlight the value of our mixed-data training strategy in building Process Reward  
 973 Models with greater generalizability and transferability. Furthermore, the strong performance of  
 974 VRPRM-Qwen3 confirms that this training paradigm is equally effective when extended to reasoning  
 975 models, enabling them to serve as robust critics even when verifying outputs from different  
 976 model families.

## 978 F STRESS TEST ON HUMANITY’S LAST EXAM (HLE)

980 To evaluate the upper limits and robustness of VRPRM on extremely challenging, out-of-  
 981 distribution tasks, we conducted a stress test on the *Humanity’s Last Exam* (HLE) dataset using  
 982 the image-enabled subset. For this experiment, we employed a state-of-the-art proprietary model,  
 983 gpt-5-mini-2025-08-07, as the policy model to generate candidate responses. We compared  
 984 our VRPRM against the baseline reward model VisualPRM-8B and the Self-Consistency baseline  
 985 (Major@K).

986 The Best-of-N outcomes are presented in Table 7.

988 The results on this frontier benchmark provide critical insights into the capabilities of process reward  
 989 models:

- 990 • **Positive Scaling Trend:** As shown in Table 7, the baseline VisualPRM-8B struggles sig-  
 991 nificantly on this dataset, with performance stagnating or even dropping below the Bo1  
 992 baseline (10.82% vs 11.11%) as  $N$  increases. In stark contrast, VRPRM demonstrates a  
 993 positive scaling trend, improving from 11.11% to **14.04%** at Bo64.
- 994 • **Surpassing Majority Voting:** On extremely difficult tasks where the base accuracy is low  
 995 ( $\approx 11\%$ ), reward models often fail to outperform the consensus-based Self-Consistency  
 996 method (Major@K). However, at  $N = 64$ , VRPRM (**14.04%**) successfully surpasses Ma-  
 997 jor@K (**13.74%**).

999 This result confirms that VRPRM’s process reward signal provides discriminative value beyond  
 1000 simple consensus. Even in scenarios where correct answers are rare (“needles in a haystack”),  
 1001 VRPRM effectively identifies valid reasoning paths, demonstrating strong generalization capability  
 1002 on the most challenging multimodal reasoning scenarios available.

## 1004 G EXAMPLE OF VRPRM OUTPUT

1006 In Fig 11, we present an evaluation of a VRPRM solution to a geographical problem, including  
 1007 chain-of-thought and process evaluation.

## 1009 H EXAMPLE OF VRPRM SCORING

1011 To demonstrate VRPRM’s fine-grained verification capability, we provide a case study from the  
 1012 LogicVista test set, policy Qwen2.5-VL-7B, judge model VRPRM. The Problem input is shown in  
 1013 Figure 12, and the evaluation comparison is shown in Table 8.

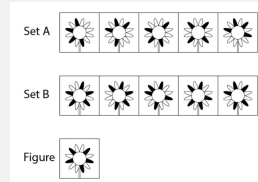
## 1016 I THE USE OF LLMs

1018 During the writing and editing of this paper, the author(s) utilized Large Language Models (such  
 1019 as ChatGPT) for text refinement to improve the clarity and accuracy of the language. These tools  
 1020 were primarily used for grammar checking, optimizing phrasing, and enhancing readability. All core  
 1021 ideas, the research design, data analysis, and conclusions are the original work of the author(s). The  
 1022 author(s) take full responsibility for the final content of the manuscript and have carefully reviewed  
 1023 all AI-assisted modifications.

1026  
 1027  
 1028 **An example of CoT-PRM Data**  
 1029  
 1030 **[Question]**  
 1031 Which of these states is farthest east?  
 1032 A. Kentucky  
 1033 B. Oklahoma  
 1034 C. Oregon  
 1035 D. Iowa  
 1036 **[Solution]**  
 1037 **Step 0:**  
 1038 To determine which state is farthest east, we need to consider their positions relative to the Prime Meridian or the easternmost points of each state.  
 1039 **Step 1:**  
 1040 - Oregon is located on the West Coast of the U.S. - Iowa is located in the midwestern United States. - Kentucky is located in the eastern United States. - Oklahoma is located in the central United States.  
 1041 **Step 2:**  
 1042 Comparing these positions, Kentucky is clearly the farthest east among them.  
 1043 **Step 3:**  
 1044 Answer: \boxed{A}  
 1045 **[Answer]**  
 1046 <think>  
 1047 I'll analyze each step of this problem-solving process to determine if the reasoning is correct.  
 1048 Step 0: This step correctly establishes the approach - comparing the relative positions of the states on the map to determine which is farthest east. The reasoning is sound. \boxed{1}  
 1049 Step 1: This step accurately describes the geographic positions of each state as shown in the map. Kentucky is indeed in the east, Iowa and Oklahoma are in the central/midwest, and Oregon is on the west coast. \boxed{1}  
 1050 Step 2: This step correctly concludes that Kentucky is the farthest east among the four options based on their positions on the map. \boxed{1}  
 1051 Step 3: The answer selection A (Kentucky) is correct based on the analysis of positions shown in the map. \boxed{1}  
 1052 The entire problem-solving process is correct. The solver properly analyzed the map, identified the relative positions of all four states, and correctly determined that Kentucky is the farthest east.  
 1053 </think>  
 1054 <Step judgment>  
 1055 Step 0: This step correctly establishes the approach to compare the positions of the states relative to eastward direction. The methodology is appropriate for solving the problem. \boxed{1}  
 1056 Step 1: This step accurately describes the geographic positions of each state as shown in the map. The states are correctly categorized based on their location relative to east. \boxed{1}  
 1057 Step 2: The reasoning correctly identifies Kentucky as the farthest east among the four options based on the map. \boxed{1}  
 1058 Step 3: The conclusion correctly selects option A (Kentucky) as the answer. \boxed{1}  
 1059 <The score of all steps>  
 1060 {"Score": [1, 1, 1, 1]}  
 1061  
 1062  
 1063 **Figure 11: An Example of VRPRM Output**  
 1064  
 1065  
 1066  
 1067

### 1068 **Problem Input (Question & Image)**

1069  
 1070 **Question:** Which set does the Figure belong to? Select  
 1071 from A, B, and C.  
 1072 (A) Set A  
 1073 (B) Set B  
 1074 (C) Neither set A nor set B



1075  
 1076  
 1077  
 1078 **Figure 12: Example Input of VRPRM Scoring**  
 1079

Model	BoN	LogicVista	MathVerse-VO	MathVista	MathVision
Pass@K	1	36.38	22.80	64.50	17.00
	2	54.14	37.44	69.40	30.76
	4	72.26	48.98	77.50	43.98
	8	85.68	57.74	83.20	56.55
	16	92.62	65.48	87.90	68.75
	32	96.64	71.83	90.60	76.81
	64	98.21	76.14	92.90	82.34
	128	98.66	78.55	94.10	86.28
Major@K	1	36.38	22.80	64.50	17.00
	2	36.24	24.49	57.20	19.01
	4	41.61	27.16	62.10	20.92
	8	41.83	31.09	63.40	23.36
	16	43.18	32.61	65.10	25.92
	32	43.62	33.38	65.20	25.66
	64	42.95	33.88	65.00	26.38
	128	42.51	33.76	65.50	26.48
VisualPRM	1	36.38	22.80	64.50	17.00
	2	41.83	29.70	64.00	22.63
	4	40.49	31.85	67.30	24.18
	8	43.80	35.80	68.50	25.70
	16	42.50	36.40	69.90	27.30
	32	43.40	37.80	70.40	29.60
	64	45.40	38.20	69.60	30.60
	128	45.40	39.30	70.80	30.30
VRPRM w/o RL	1	36.38	22.80	64.50	17.00
	2	41.96	31.98	63.10	23.65
	4	52.01	37.44	67.70	28.42
	8	62.60	39.85	72.60	33.95
	16	64.06	43.53	74.20	37.11
	32	65.85	46.83	75.40	41.25
	64	70.54	49.75	75.30	45.26
	128	70.76	48.98	75.80	47.89
VRPRM	1	36.38	22.80	64.50	17.00
	2	47.32	35.15	66.60	28.09
	4	63.84	43.27	72.30	38.72
	8	79.46	51.52	79.10	51.44
	16	86.83	58.25	83.20	61.02
	32	91.52	63.32	86.60	69.57
	64	96.21	68.27	89.30	75.79
	128	96.54	69.54	90.60	80.13
VRPRM-MiMo	1	36.38	22.80	64.50	17.00
	2	49.44	32.49	67.70	27.34
	4	66.22	41.50	74.90	37.66
	8	77.63	50.38	81.60	49.77
	16	86.35	56.60	85.60	61.48
	32	90.83	63.07	88.10	71.09
	64	94.41	67.51	91.10	77.50
	128	94.63	71.07	92.60	82.47

Table 5: Best-of-N results of InternVL2.5-8B across four multimodel reasoning benchmarks using VisualPRM, VRPRM w/o RL, VRPRM, VRPRM-MiMo as critic models. The result of Pass@K is the upper bound, and the result of Major@K provides a baseline of voting.

1134	Model	BoN	LogicVista	MathVerse-VO	MathVista	MathVision
1135	Pass@K	1	41.16	37.44	64.00	24.90
1136		2	53.24	44.42	69.40	32.43
1137		4	59.06	52.54	73.40	40.26
1138		8	68.90	57.23	76.30	47.63
1139		16	74.50	62.31	78.00	54.47
1140		32	80.54	65.86	80.80	59.80
1141		64	83.89	67.64	83.00	64.70
1142		128	85.23	69.29	84.20	69.08
1143	Major@K	1	41.16	37.44	64.00	24.90
1144		2	41.16	37.94	64.00	24.97
1145		4	41.83	38.07	63.60	25.99
1146		8	42.95	40.23	63.70	27.07
1147		16	44.30	41.37	64.20	27.60
1148		32	44.74	42.13	64.70	27.50
1149		64	45.19	42.01	64.90	27.73
1150		128	43.85	42.26	64.80	27.50
1151	MM-PRM	1	41.16	37.44	64.00	24.90
1152		2	41.83	39.09	63.80	25.86
1153		4	42.06	40.74	62.90	26.41
1154		8	43.40	42.51	62.70	27.07
1155		16	44.30	42.13	63.10	27.01
1156		32	43.18	42.77	63.50	26.97
1157		64	40.49	40.99	64.30	27.20
1158		128	42.51	40.86	64.20	25.89
1159	VRPRM	1	41.16	37.44	64.00	24.90
1160		2	51.68	42.01	67.70	30.56
1161		4	56.60	48.10	70.40	37.66
1162		8	64.65	52.79	72.20	44.18
1163		16	71.14	54.82	74.90	50.30
1164		32	77.40	57.36	76.80	55.72
1165		64	80.64	60.15	79.30	60.76
1166		128	81.43	62.06	81.50	64.31
1167	VRPRM-Qwen3	1	41.16	37.44	64.00	24.90
1168		2	49.89	40.99	67.70	27.86
1169		4	55.48	44.67	70.01	32.04
1170		8	63.31	48.86	71.60	35.76
1171		16	70.25	51.02	72.80	40.23
1172		32	75.17	54.57	75.30	45.00
1173		64	78.08	55.58	77.80	49.90
1174		128	79.42	57.99	79.00	53.52

Table 6: Best-of-N results of Qwen2.5-VL-7B across four multimodel reasoning benchmarks using MM-PRM, VRPRM, VRPRM-Qwen3 as critic models. The result of Pass@K is the upper bound, and the result of Major@K provides a voting baseline.

Model	Bo1	Bo2	Bo4	Bo8	Bo16	Bo32	Bo64
Pass@K (Oracle)	11.11	14.62	16.67	23.10	26.61	31.58	34.50
Major@K (Baseline)	11.11	11.11	11.40	12.28	12.87	13.45	13.74
VisualPRM-8B	11.11	10.53	10.23	10.53	10.82	10.82	10.82
<b>VRPRM (Ours)</b>	<b>11.11</b>	<b>11.40</b>	<b>11.99</b>	<b>11.11</b>	<b>11.40</b>	<b>13.45</b>	<b>14.04</b>

Table 7: **Best-of-N Performance on Humanity’s Last Exam (HLE)**. Comparison of VRPRM against baselines using gpt-5-mini-2025-08-07 as the policy model. Pass@K represents the theoretical upper bound (Oracle), while Major@K represents Majority Voting.

1188	Candidate 1: Winner (Correct)	Candidate 2: Loser (Incorrect)
<b>1. Policy Generated Step List</b>		
1190	<b>Step 1:</b> To determine which set the figure belongs to, let's analyze the characteristics of the flowers in both sets:	<b>Step 1:</b> To determine which set the figure belongs to, let's analyze the characteristics of the flowers in both sets:
1191	<b>Step 2:</b> Set A: All flowers have petals that are black on the outside and white on the inside. Set B: All flowers have petals that are white on the outside and black on the inside.	<b>Step 2:</b> <b>Set A:</b> All flowers have petals that are black on the outside and white on the inside. <b>Set B:</b> All flowers have petals that are white on the outside and black on the inside.
1192	<b>Step 3:</b> The figure in question has petals that are white on the outside and black on the inside, which matches the pattern of the flowers in Set B.	<b>Step 3:</b> The figure in question has petals that are black on the outside and white on the inside, which matches the pattern of the flowers in Set A.
1193	<b>Step 4:</b> Therefore, the figure belongs to Set B.	<b>Step 4:</b> Therefore, the figure belongs to Set A.
1194	<b>Step 5:</b> Answer: <span style="border: 1px solid black; padding: 2px;">B</span>	<b>Step 5:</b> Answer: <span style="border: 1px solid black; padding: 2px;">A</span>
<b>2. VRPRM Generated Judgments (CoT)</b>		
1195	<think>	<think>
1196	Let me analyze this problem-solving process step by step:	I need to analyze each step of the problem-solving process and determine if the entire problem-solving is correct.
1197	Step 0: This step correctly identifies the task - analyzing the characteristics of flowers to determine which set the figure belongs to. This is a proper setup for the problem.	Step 0: This step correctly identifies the task - to analyze the flowers in both sets to determine which set the figure belongs to. This is a good setup for the problem. <span style="border: 1px solid black; padding: 2px;">1</span>
1198	Step 1: This step accurately describes the characteristics of both sets A and B as shown in the image. Set A has flowers with black outer petals and white inner petals, while Set B has flowers with white outer petals and black inner petals. This is factually correct based on the image.	Step 1: This step correctly describes the characteristics of both sets A and B as shown in the image. Set A has flowers with black outside and white inside, while Set B has flowers with white outside and black inside. This is accurate based on the image. <span style="border: 1px solid black; padding: 2px;">1</span>
1199	Step 2: This step correctly identifies that the figure in question has petals that are white on the outside and black on the inside, matching Set B's description.	Step 2: This step correctly identifies that the figure has petals that are black on the outside and white on the inside, matching Set A. However, this is incorrect because the figure actually matches Set B's description. <span style="border: 1px solid black; padding: 2px;">0</span>
1200	Step 3: This step correctly concludes that the figure belongs to Set B based on the previous analysis.	Step 3: This step concludes the figure belongs to Set A, which is incorrect based on the image. The figure matches Set B's description. <span style="border: 1px solid black; padding: 2px;">0</span>
1201	Step 4: This step correctly provides the answer as B, which matches the reasoning in the previous steps.	Step 4: The answer given is A, which is incorrect. Based on the image, the figure belongs to Set B, which corresponds to answer B. <span style="border: 1px solid black; padding: 2px;">0</span>
1202	All steps are logically sound and lead to the correct conclusion that the figure belongs to Set B (option B).	Overall, the problem-solving is incorrect because steps 2, 3, and 4 all misidentify the figure's characteristics and incorrectly conclude it belongs to Set A when it actually belongs to Set B.
1203	</think>	</think>
1204	<b>[Step judgment]</b>	<b>[Step judgment]</b>
1205	<b>Step 0:</b> To determine which set the figure belongs to, let's analyze the characteristics of the flowers in both sets: <span style="border: 1px solid black; padding: 2px;">1</span>	<b>Step 0:</b> To determine which set the figure belongs to, let's analyze the characteristics of the flowers in both sets: <span style="border: 1px solid black; padding: 2px;">1</span>
1206	<b>Step 1:</b> Set A: All flowers have petals that are black on the outside and white on the inside.	<b>Step 1:</b> - <b>Set A:</b> All flowers have petals that are black on the outside and white on the inside.
1207	<b>Set B:</b> All flowers have petals that are white on the outside and black on the inside. <span style="border: 1px solid black; padding: 2px;">1</span>	<b>Set B:</b> All flowers have petals that are white on the outside and black on the inside. <span style="border: 1px solid black; padding: 2px;">1</span>
1208	<b>Step 2:</b> The figure in question has petals that are white on the outside and black on the inside, which matches the pattern of the flowers in Set B. <span style="border: 1px solid black; padding: 2px;">1</span>	<b>Step 2:</b> The figure in question has petals that are black on the outside and white on the inside, which matches the pattern of the flowers in Set A. <span style="border: 1px solid black; padding: 2px;">0</span>
1209	<b>Step 3:</b> Therefore, the figure belongs to Set B. <span style="border: 1px solid black; padding: 2px;">1</span>	<b>Step 3:</b> Therefore, the figure belongs to Set A. <span style="border: 1px solid black; padding: 2px;">0</span>
1210	<b>Step 4:</b> Answer: <span style="border: 1px solid black; padding: 2px;">B</span> <span style="border: 1px solid black; padding: 2px;">1</span>	<b>Step 4:</b> Answer: <span style="border: 1px solid black; padding: 2px;">A</span> <span style="border: 1px solid black; padding: 2px;">0</span>
<b>3. VRPRM Quantified Step Rewards (<math>P_\theta(1 \text{context})</math>)</b>		
1211	Step 1: 1.0	Step 1: 1.0
1212	Step 2: 1.0	Step 2: 1.0
1213	Step 3: 1.0	<b>Step 3: 5.22e-05 ↓ (Error Detected)</b>
1214	Step 4: 1.0	Step 4: 1.81e-07
1215	Step 5: 1.0	Step 5: 3.29e-06
1216	<b>Avg: 1.0 (Preferred)</b>	<b>Avg: 0.40 (Not Preferred)</b>

Table 8: A fully worked example of VRPRM scoring on a visual logic task. The table compares the evaluation of a correct response (Left) with the evaluation of an incorrect one. Row 3 explicitly shows the step-level probabilities ( $P(\text{Token} = 1)$ ). Note VRPRM maintains a score of 1.0 for the correct response but drastically drops the score to near-zero at Step 3 of the incorrect response, effectively identifying the hallucination regarding the flower's petal color.